Jinlong Zhao, Xinjiang Li, Zhenqi Hu, Rongxue Kang, Grunde Jomaas,

Experimental study of the burning behavior and key parameters of gasoline pool fires with different ullage heights,

Fire Safety Journal,

Volume 140,

2023,

103912,

ISSN 0379-7112

The article has been published in final form at:

https://doi.org/10.1016/j.firesaf.2023.103912

Experimental study of the burning behavior and key parameters of gasoline pool fires with different ullage heights

Jinlong Zhao[a,b], Xinjiang Li[a], Zhenqi Hu[a], Rongxue Kang[a,b]*, Grunde Jomaas[c]

a. China University of Mining & Technology, Beijing, Beijing, 100083, China

b. China Academy of Safety Science and Technology, Beijing, Beijing 100012, China

c. FRISSBE, Slovenian National Building and Civil Engineering Institute (ZAG), 1000, Ljubljana, Slovenia

Highlights:

- The burning behavior of the radiation-controlled pool fires under different ullage heights is analyzed experimentally.
- Dimensionless down-reaching flame length (L_{down}*) increases exponentially with the increase of h*.
- A new correlation is established to predict the steady burning rate for pool fires with different ullage heights.

Abstract:

Pool fires with different ullage heights are a common type of fire accident. A series of gasoline pool fire experiments with two sizes (D = 40 cm, 60 cm) and six ullage heights (h = 0, 0.2D, 0.4D, 0.6D, 0.8D, 1.0D) are conducted. The burning process, axial temperature profile, radiative heat feedback, and burning rate are measured and analyzed. The result shows that the fuel vapor layer and the down-reaching flame layer are distinguished based on the axial temperature profile for the steady burning stage. Meanwhile, the down-reaching flame length (L_{down}) increases more profoundly for large tank diameters under the same ullage height. Subsequently, the dimensionless down-reaching flame length ($L_{\mathrm{down}}^* = L_{down}/D$) increases exponentially with the dimensionless ullage heights ($h^* = h/D$). Finally, based on the classical burning rate model for the low ullage height and the heat transfer process from the flame to the fuel surface, a correlation with different ullage heights is established to calculate the burning rate, which is then validated against the experimental data in the paper and literature values. The results are of importance to understand the burning rate and the radiative heat feedback to the fuel surface for pool fires with different ullage heights.

Keywords: pool fires; ullage height; down-reaching flame; flame radiative heat feedback; burning rate correlation

1. Introduction

Despite the massive focus on other forms of energy provision, liquid fuels still play an important role in energy consumption and supply [1]. In order to store large quantities of liquid fuels, some floating-roof tanks have been built and are widely used [2]. During the storage process, the fuel level will change with the variation of the fuel storage volume, followed by the different vertical distances between the fuel surface and the tank upper rim (ullage height, h). For a low liquid level, the flammable fuel vapor easily accumulates above the fuel surface, which increases the fire risk. In case of a pool fire accident, the flame will enter into the tank due to the restriction of air entrainment by the ullage height, which further affects the fire accident evolution. There are several tank fires occurring worldwide every year [3]. For example, a storage tank fire accident occurred at Dalian, Liaoning Province, China in 2011[4]. The flame entered the tank because of the low liquid level, which eventually caused the collapse of the sidewall. Understanding the role played by the ullage height is one of the aspects that are of importance for reducing the risk associated with storing liquid fuels in tanks.

The burning behavior of pool fire with different ullage heights have been investigated in the past. More than 50 years ago, Blinov and Khudyakov [5] conducted some experiments ($0.56 \leq D \leq 2.26$ cm) to analyze the ullage height effect and found that the burning rate decreased with the increase of the ullage height. Shi et al. [6] also conducted some small scale (D = 2.5 cm and 5 cm) methanol pool fire experiments in a cavity. They pointed out that there was a given ullage in which the burning rate reached a minimum value. Then some numerical simulations were used to complement the results and showed that the down-reaching flame appearance resulted in the mass burning rate increasing again with the ullage height. Moreover, a series of large experiments (D = 1–1.5 m, h = 10-20 cm) were also conducted to develop an understanding of the burning of crude oil. They demonstrated that the burning rate increased with the ullage height because a fire induced air entrainment into the cavity formed a recirculation zone that premixed the oil vapor with the air, which resulted in a significant increase in flame heat feedback to the oil surface [7]. Kolstad et al. [8] experimentally studied the ullage height effect on the burning rate of pool fire with some relatively large diameters (D = 10, 20, 30 cm). In their study, they found that the burning rate was affected by the lip height enough for it to surpass the diameter effect. Kuang et al. [9] presented an experimental investigation into the pool fire burning rates with different lip heights under the different cross flow air speeds. They observed that the cross flow affected the burning rate, especially for the larger ullage height. In order to find the reasons for the burning rate variations with ullage heights, the flame heat feedback has been studied by some scholars. Liu et al. [10] investigated the ullage height effects on the heat feedback. They found that the incident radiative heat flux to the fuel surface fraction first increased and then decreased with ullage height while the convective heat feedback fraction presented a reverse trend. This was attributed to the flame base suspension and the soot evolution due to incomplete combustion. Huang et al. [11] carried out some pool fire experiments (D = 10-20 cm) using *n*-heptane and ethanol to investigate ullage height (0 until the burning could not be sustained) effects on the heat transfer and combustion characteristics. They found that the radiative heat feedback rate generally decreased for the fuels, while the convective heat feedback rate increases slightly, followed by a decrease with h/D. Moreover, a mass flux correlation based on the modified stagnant film theory was developed for the convection-dominated pool fires. In addition to studies of the burning rate and heat feedback for pool fires with different ullage heights, the flame behavior has also been studied by some scholars. He et al. [12] experimentally studied the flame height variations with the ullage height by using steel trays and a new correlation for upper flame height was established by considering the ullage height, tray diameter, and heat release rate. Zhang et al. [13] presented two oil pool fires experiments under different ullage heights to investigate the upper flame height evolution. They demonstrated that the upper flame height first increased and then decreased with the ullage height increase and eventually reached a local maximum value. This was attributed to the strengthened vortex around the sidewall rims by the ullage height, which initially resulted in an increase in air entrainment. Zhao et al. [14] conducted a series of pool fire tests by four transparent glass trays (L = 20-35 cm) with different ullage heights, in which the total flame was observed and divided into the two parts: a down-reaching flame and an upper flame. They then developed a theoretical model for the total flame length. Liu et al. [15] studied the ullage height ($0 \leq h/D \leq 1$) effect on the flame behavior using both experimental and numerical (FDS) methods. They found that there was a negative pressure region in the tank which resulted in the surrounding air entrance into the pool, forming the down-reaching flame. The above studies clearly indicate that the ullage height significantly affects the burning rate, the flame heat feedback to the fuel surface and the flame behavior, which even surpass the diameter effects. Although both the flame heat feedback to the fuel surface and the flame behavior are analyzed to explain the lower burning rate for the cases with large ullage heights, previous studies are predominantly qualitative in nature. Currently, there is no available model to calculate the burning rate for the radiation-controlled pool fires under different ullage heights. Furthermore, most of the experiment data are from some small-scale experiments ($D \leq 20$ cm), in which the burning rate is controlled by the conduction or convection [16], far from the practical accidents. Therefore, the experimental data of the whole burning process and burning rates for large ullage height pool fires controlled by radiation are still limited.

Motivated by the above discussions, this study is aimed at investigating the burning characteristics of pool fires with different ullage heights. A series of experiments were performed using two customized tanks with different ullage heights. The burning rate, temperature profiles in the tank, and radiative heat feedback to the fuel surface were measured and analyzed.

2. Experimental setup and models

2.1. Experimental setup

A schematic of the experimental setup is shown in Fig. 1. Two custom-made circular trays with diameters (D) of 0.4 m and 0.6 m were used, and the corresponding sidewall height was 60 cm and 80 cm, respectively. The sidewalls and the bottom of the custom-made circular trays were made of stainless (with a thickness of 2.5 mm). The position of the circular trays could be adjusted by a supporting device so that the ullage height could be accurately confirmed, as shown in Fig.1(b). The circular tray was placed on an electronic balance (maximum load: 150 kg, accuracy: 0.1 g) to measure the real-time fuel mass so that the mass burning rate can be calculated. The burning process was recorded by a digital video camera.

The A series of K-type thermocouples (diameter: 1 mm) were placed along the centerline to measure the temperature in the tank, for which the distance between two nearby thermocouple pairs was 2 cm, as shown in Fig. 1(c). A heat flux meter (SGB) was used to measure the flame's radiative heat flux to the fuel surface. A quartz glass tube (thickness: 2 mm, transmissivity: 0.82) was positioned at the bottom to protect the heat flux meter, as shown in Fig.1(d). This measure was widely used in fire experiments [11].

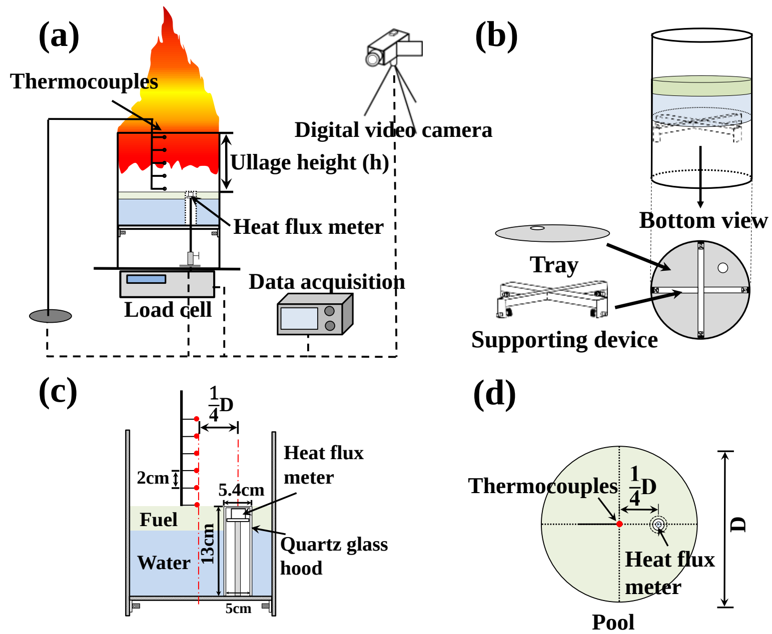

Fig. 1. Schematic of the detailed experimental setup.

In order to reduce the influence of wind speed on the burning process, the experiments were carried out in a semi-enclosed space. Before the experiments, a water layer (thickness: 11 cm) was injected into the tray to prevent the bottom of the tray from overheating and deformation. The fuel used in the experiments was gasoline (92 octane), with an initial fuel layer thickness of 2 cm, for which the burning lasted at least 3 min after reaching steady burning. The detail experimental specifications are shown in Table 1. Note that each of the 12 test conditions was carried out at least 3 times.

Table1. Overview of the experimental conditions.

Test No.	Diameter (cm)	height (cm)	*h/D*	Initial fuel layer thickness (cm)
1	40	0	0	2
2	40	8	0.2	2
3	40	16	0.4	2
4	40	24	0.6	2
5	40	32	0.8	2
6	40	40	1.0	2
7	60	0	0	2
8	60	12	0.2	2
9	60	24	0.4	2
10	60	36	0.6	2
11	60	48	0.8	2
12	60	60	1.0	2

2.2. Burning rate model in pool fire with small ullage heights

For pool fires, the heat flux ($\dot{q}_f$) received by the fuel surface mainly includes three parts: the conductive heat from the sidewall to the fuel, the convective heat from the gas above the liquid surface and the radiative heat from the flame to the fuel surface, which can be expressed as follows [17]:

$$\dot{q}_f = \frac{4k(T_r - T_l)}{D} + h(T_g - T_l) + \sigma F(T_f^4 - T_l^4)(1 - \exp(-k^{'} D)) \tag{1}$$

where k, h and σ are the conduction heat transfer coefficient, convection heat transfer coefficient and Stefan-Boltzmann constant, respectively; k' is a constant, which equals to the extinction coefficient multiplied by the mean beam length corrector ($k\beta$) [16]; D is the tray diameter; F is the view factor; and T_r, T_g, T_f, and T_l are the temperatures of the tray rim, liquid gas above the liquid surface, flame, and liquid fuel, respectively; T_l is the liquid fuel boiling point.

For the radiation-controlled burning (D > 20 cm), the flame heat feedback to the fuel surface can be simplified as [17]:

$$\dot{q}_f = \sigma F(T_f^4 - T_l^4)(1 - \exp(-k'D)) \tag{2}$$

Then the burning rate ($\dot{m}$) can be written as:

$$\dot{q}_f = \dot{m}(c_p(T_{boil} - T_\infty) + L_v) \tag{3}$$

where c_p is the specific heat at constant pressure, L_v is the latent heat of vaporization, and T_{boil} and T_∞ are the fuel boiling point and ambient temperature, respectively. For the fuel burning, the fuel surface temperature usually keeps the boiling point to sustain the burning ($T_l = T_{boil}$).

Combining Eqs (1-3), the burning rate can be expressed as:

$$\dot{m} = \frac{\sigma F(T_f^4 - T_l^4)}{c_p(T_{boil} - T_\infty)}(1 - \exp(-k'D)) = \dot{m}_\infty(1 - \exp(-k'D)) \tag{4}$$

where $\dot{m}_\infty$ is the mass burning rate of a pool fire with an infinite tray diameter. The burning rate of most fuels with a diameter larger than 1 m can be approximated as the maximum burning value ($\dot{m}_\infty$) [16].

3. Results and discussion

3.1. Burning process

Figure 2 shows some typical flame shapes for different ullage heights (for the cases with D = 60 cm: (a) h^* = 0; (b) h^* = 1.0). After the ignition, the flame length increases rapidly, after which the flame height remains steady for a long period. Near the end of the test, the flame height decreases rapidly, and the flame re-enters the tray as the fuel is depleted. Meanwhile, comparing Fig. 2 (a) and (b), it is clear that the larger the ullage height, the lower the steady flame height of the pool fires.

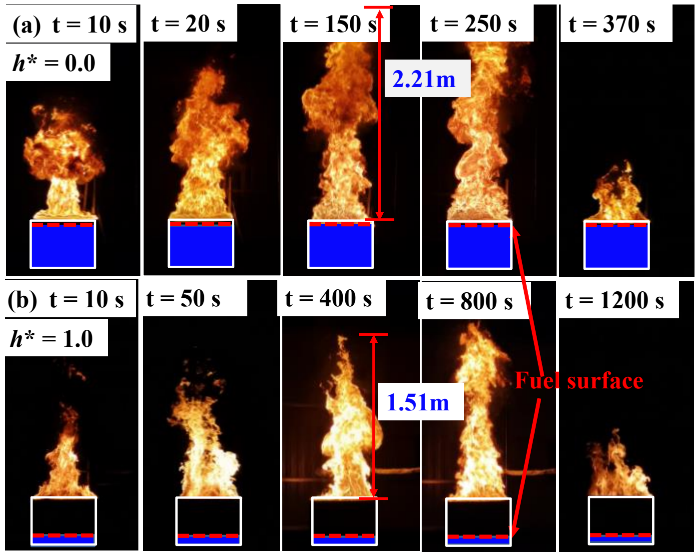

Fig. 2. Typical flame shapes at different times for the case D = 60 cm: (a) h^* = 0; (b) h^* = 1.0. Note that, apart from the first photo, the frames are taken at different times for the two conditions.

In order to further show the whole burning process, the transient burning rates of pool fire (D = 60 cm) with different ullage heights are shown in Fig. 3. The burning rate shows a tendency to increase first, gradually stabilize and finally decrease. The variation of the mass burning rate is consistent with that of the flame height. Meanwhile, it is also found that the mass burning rate of the pool fire with h^* = 1.0 is lower than that with h^* = 0, which directly indicates that the ullage height has a significant influence on the mass burning rate. Considering Figs. 2 and 3, it is useful to divide the burning process into three typical stages: (1) initial stage, (2) steady burning stage and (3) extinguishment stage.

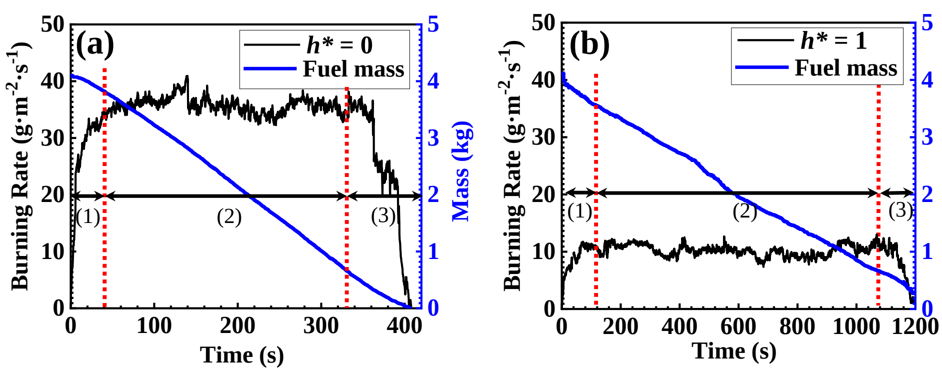

Fig. 3. Experimental data of burning rate and fuel mass for different ullage height vs. burning time (D = 60 cm: (a) h^* = 0; (b) h^* = 1.0).

The axial temperature profile in the tank is related to the burning behaviors. In Fig. 4(a), Test 12 (D = 60 cm, h^* = 1.0) is used as an example to show the temperature variation. Fig. 4(b) then shows the radiative heat feedback from the flame to the fuel surface in Test 9 (h^* = 0) and Test 12 (h^* = 1.0) against the non-dimensional time.

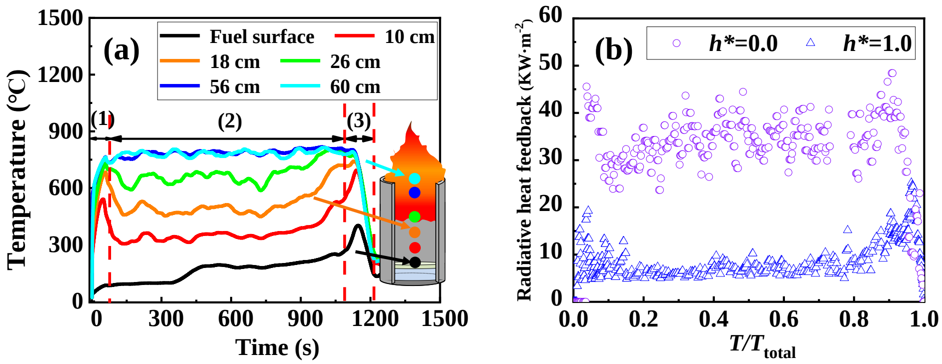

Fig. 4. (a) Axial temperature profile in the vertical direction at different times (h^* = 1.0, D = 60 cm); (b) The radiative heat feedback from the flame to the fuel surface for different ullage heights (h^* = 0, 1.0, D = 60 cm) against the non-dimensional time.

In Fig. 4, it can be observed that, as expected, the axial temperature in the tank increases rapidly at the initial stage, up to around 700 °C, which is accompanied by the flame radiative heat feedback. This is because the flame is mainly located in the tank due to the oxygen existence after the ignition of fuel. However, as the burning continues, the inner temperature gradually drops, especially near the fuel surface, from around 700 °C to 300 °C. This shows that the flame base gradually moves up because of the restricted air entrainment by the sidewall. Meanwhile, this process has also been observed in the previous experiments using the transparent quartz glass trays [14]. In addition, the variations in the radiative heat feedback from the flame to the fuel surface in Fig. 4(b) further illustrates the flame lifting process in the initial stage. For the steady burning stage, the axial temperature profile in the tank and the radiative heat feedback are basically stable. Combined with the axial temperature profile, it can be seen that the space in the tank can be divided into two layers: (i) fuel vapor layer (the fuel surface to the flame base) and (ii) the down-reaching flame layer (the flame base to the tank upper rim) in the steady burning stage. For the extinguishment stage, it is found that both the axial temperature in the tank and the radiative heat feedback increases first in a short time. This can be attributed to the lower burning rate that causes the flame re-entered into the tank. Then, the axial temperature and the radiative heat feedback decrease rapidly until to small values because of the disappearance of the flame. It is noted that the measured radiative heat feedback is mainly from the hot tube and the sidewall surface, after the fire extinguishment. This measured value was less than 1 kW/m^2. As a result, the influence of the glass surface is considered to be insignificant enough to be neglected.

3.2. Axial temperature profile at the steady burning stage

In order to further analyze the steady axial temperature profile in the tank, Fig. 5 shows the axial temperature profile of the pool fires (D = 40 cm) for h = 32 cm and h = 40 cm.

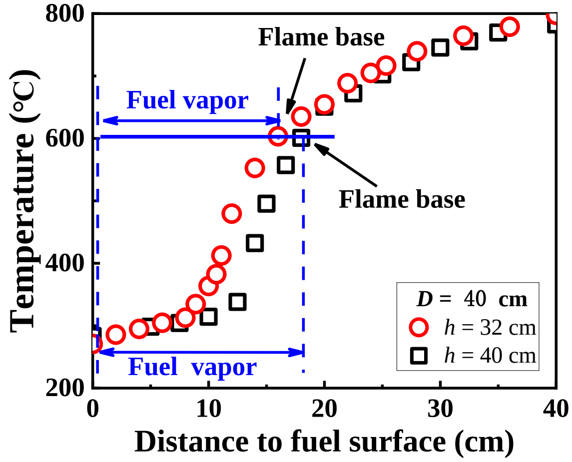

Fig. 5. The axial temperature profile for steady burning with different ullage heights for the case D = 40 cm.

According to Fig. 5, as the distance increases to the fuel surface, the temperature begins to increase slowly first, especially near the fuel surface. This is mainly because this part is far from the flame. As the distance increases, the temperature increases sharply to around 600 °C. This region is directly affected by the down-reaching flame. In comparison with previous pool fire experiments with glass trays, it is found that the temperature is about 600°C [18] at the boundary between the fuel vapor and flame (the flame intermittency of 0.5). Based on this finding, the fuel vapor layer and the down-reaching flame layer can be distinguished. In Fig. 5, the thickness of the fuel vapor is also determined and it can be seen that the fuel vapor thickness increases with h*. This is mainly because of the greater air entrainment restriction imposed by the higher sidewall, which results in flame base rise. Fig. 6 shows the down-reaching flame as a function of h* and a correlation of the length of down-reaching flame and dimensionless ullage height at the steady burning stage, respectively.

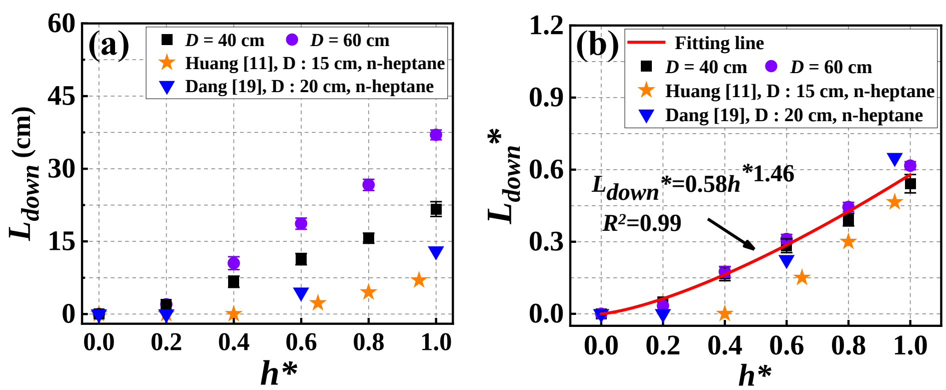

Fig. 6. A correlation of down-reaching flame length and dimensionless ullage height in the steady burning stage.

By inspecting Fig. 6(a), it can be found that L_{down} increases with h*. Meanwhile, L_{down} increases more pronouncedly for the large tanks because of the increased air entrainment associated with flame sizes [14]. Fig. 6(b) shows that the dimensionless down-reaching flame length increases exponentially with the increase of h*, which is consistent with the findings by Dang et al. [19]. Meanwhile, L_{down}^{*} is almost independent on the pool diameter for the radiation-controlled burning (D > 20 cm). To predict the L_{down}, an empirical equation has been proposed by Dang et al. [19] ：

$$L_{D,down} / D = a \times h^{*b} \tag{5}$$

Combined with the experimental data, L^*_{down} can be expressed as:

$$L^*_{D,down} = 0.58 \times h^{*1.46} \tag{6}$$

In Fig. 6, it can be found that there is a good agreement between the measurements and the prediction with a fitting coefficient (R^2>0.99), which verifies that the correlation can predict the down-reaching flame length very well. In order to further enrich the experimental data and analyze the sidewall influence, Fig. 6 also adds the down-reaching flame length data presented in the studies by Huang et al. and Dang et al. [11, 19]. It should be noted that some experiment data cannot be obtained in these scholar studies. So only parts of experiment data were selected and added in Fig.6. By comparison, it is found that the developed correlation can also predict the down-reaching flame length. However, it is noted that there is a certain deviation for those from the work by Huang et al., especially the cases with the lower sidewall. This is mainly because of the stronger heat conduction from the sidewall for the small-scale burning, which results in the smaller down-reaching flame length [20].

3.3. Radiative heat feedback in the steady burning phase

Figure 7 presents the steady radiative heat feedback from the flame to the fuel surface for the different dimensionless ullage heights.

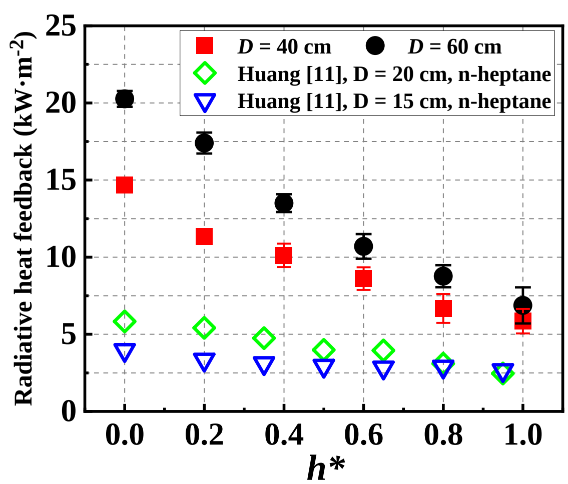

Fig. 7. Average radiative heat feedback versus h^* at the steady-state stage.

As shown in Fig.7, the radiative heat feedback (q_{rad}) from the flame to the fuel surface decreases with h^*. For the q_{rad} (kW/m^2), a solid flame model is widely used, in which the flame is considered as a cylinder and the radiation is emitted entirely from the flame surface [21]:

$$q_{rad} = E_f F_{1,2} \tau \tag{7}$$

where $F_{1,2}$ is a view factor between the flame base and the fuel surface; τ is the atmospheric transmissivity, approximately considered to be 1 for near the target [22]; and E_f is the emissive power from the flame surface. As the ullage height increases, the flame base will lift, followed by the decrease of $F_{1,2}$, which eventually causes the decrease of the radiation heat feedback to the fuel surface.

In order to analyze the effect of the pool size on the radiative heat feedback, the experimental values from the pool fire experiments with the pool diameters of 15 cm and 20 cm by Huang et al. [11] are also plotted in Fig. 7. It can be observed that the radiative heat feedback is smaller than the ones measured in our study, which is a result that is consistent with those for the pool fires with lower ullage height [23]. This is because the tank size is small, followed by the weak radiative heat feedback. Meanwhile, the decreased rate of the radiative heat feedback in the study by Huang et al. is not obvious, which is probably due to the effect of radiative heat feedback to the fuel surface from the high-temperature sidewall.

3.4. Steady burning rate and modeling

Figure 8 shows the steady burning rate as a function of the ullage height. The burning rate decreases gradually with an increase of the h^* for the same pool diameter, which is consistent with the tendency of the radiative heat feedback to the fuel surface in Fig. 7. For the same ullage height, the burning rate tends to increase with the pool diameter. This can be explained by the fact that the radiative heat feedback increases with the tank diameter, as shown in Fig. 7. Meanwhile, in order to display the pool diameter influence, Fig. 8 also presents the experimental data from the literature [11, 24]. It confirms that the burning rate also decreases with the ullage height, which is consistent with the finding in the paper [4]. Furthermore, it can be observed that the burning rate also depends on the pool diameters, showing an increasing trend. However, there is a still difference in the burning rate for the cases with the pool diameter of 60 cm between Chen et al.'s experiments and the current experimental results. This is possibly because of the wind effect caused by an exhaust hood in Chen et al.'s experiments, which has a significant impact on the flame [9].

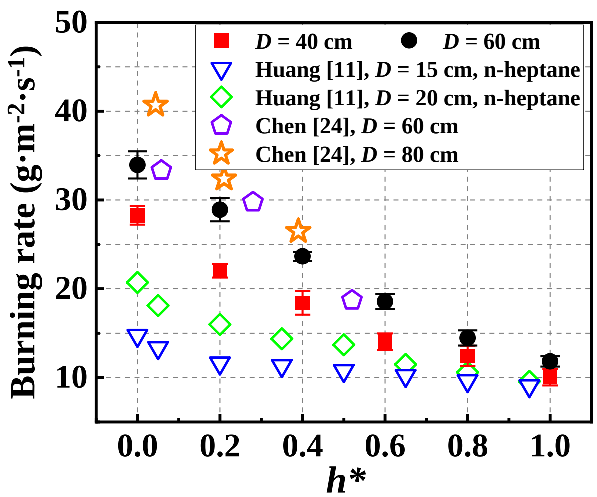

Fig. 8. Burning rates versus h^* at the steady burning stage.

For the radiation-controlled pool fires with a low ullage height, the burning rate is mainly determined by the radiative heat feedback from the flame to the fuel surface which is almost equal to the flame base. For a large ullage height, the flame radiative heat feedback can be simplified into two parts: (1) Flame radiative heat feedback to the flame base; (2) Radiation from the flame base to the fuel surface, as shown in Fig. 9.

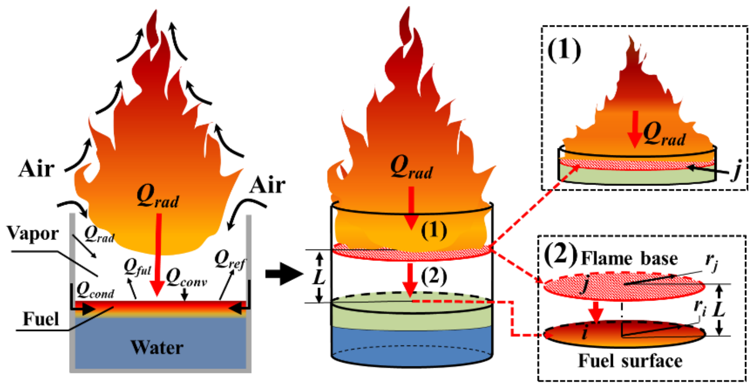

Fig. 9. Illustrations of the flame radiative heat feedback and the heat transfer process simplifications. (1) Flame radiative heat feedback to the flame base; (2) Radiation from the flame base to the fuel surface.

The radiative heat feedback to the flame base can be considered a constant as long as the flame is tall (flame height > 2*D*) and does not change color during the burning process [25]. Also, the effect of flame shape variation on the flame radiative heat feedback is negligible. Therefore, the radiative heat feedback to the flame base for the different ullage heights approximately equals the flame radiative heat feedback to the fuel surface for the low ullage height pool fires. As a result, for pool fires with different ullage heights, the $\dot{q}_f$ (kW/m^2) to the flame base can be expressed as:

$$\dot{q}_f = \dot{m}(1-\exp(-k^{'}D))(c_p(T_{boil}-T_\infty)+L_v) \tag{8}$$

After the radiative heat feedback to the flame base, there is still a vapor region in the tank between the flame base and the fuel surface. For this radiative transfer process, the radiation is roughly regarded as from the circular flame base to the circular fuel surface and the detail is shown in Fig. 9. For the view factor between the two parallel circular surfaces, F_{ij} can be expressed as [26]:

$$L_{vapor} = h - L_{down} \tag{9}$$

$$S = 1 + \frac{1+(\frac{r_j}{L_{vapor}})^2}{(\frac{r_i}{L_{vapor}})^2} \tag{10}$$

$$F_{ij} = \frac{1}{2}\{S - [S^2 - 4(r_j / r_i)^2]^{0.5}\} \tag{11}$$

where r_i is the fuel surface radius, r_j is the radiant surface radius, and L_{vapor} is the fuel vapor thickness.

Thus, combining Eqs. (4) and (7), the burning rate model for pool fires with different ullage heights can be expressed as:

$$\dot{m} = \dot{m}_\infty (1 - \exp(-k^{'} D)) F_{ij} \tau \tag{12}$$

Substituting Eqs. (3) and (8-11) into Eq. (12), the final expression of burning rate prediction model for pool fires with different ullage heights can be obtained:

$$\dot{m} = \dot{m}_\infty (1 - e^{-k'D}) \left(1 + 2(h^* - a \times h^{*b}) - 2(h^* - a \times h^{*b}) \sqrt{1 + (h^* - a \times h^{*b})} \right) \tau \tag{13}$$

In Eq. (13), the fuel vapor absorption on the flame radiative heat feedback is not considered and $\tau = 1$. For the burning rate prediction model of radiation-controlled gasoline pool fires, it can be obtained by combining Eqs. (6) and (13):

$$\dot{m} = 55(1 - e^{-1.8D}) \left(1 + 2(h^* - 0.58 \times h^{*1.46})^2 - 2(h^* - 0.58 \times h^{*1.46}) \sqrt{1 + (h^* - 0.58 \times h^{*1.46})^2} \right) \tag{14}$$

where $\dot{m}_\infty$= 55 g/(m^2·s), k' = 1.8 m^{-1} for gasoline pool fires [16]. Fig. 10 shows the comparison of calculated burning rate prediction model and experimental data in current paper and some literature values [11 14, 20, 24].

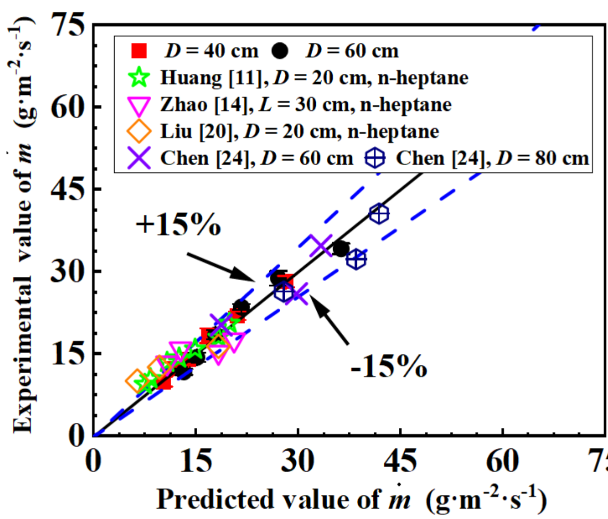

Fig. 10. Comparison of experimental and calculated burning rate using Eq. (14) and experimental data in this work and from literature.

In Fig. 10, it can be observed that the burning rate can be predicted well by the model for the cases with different ullage heights. The predictive deviation of the model may be due to the difficulty in determining the down-reaching flame heights. Furthermore, it can be found that the deviation increases for the cases with large ullage heights, which can be explained by the fact that the radiative heat feedback to the flame base is not steady, even the change in flame color for the cases with some large ullage heights [14,20]. For example, when h^* is greater than 1.5, the flame will become unstable and even extinguish [20], and the flame color also tends to blue

[14]. Therefore, it should be noted that the developed model is applicable for the stable pool fires with different ullage heights.

4. Conclusion

A series of gasoline pool fire experiments with different pool diameters and ullage heights are carried out. The entire burning process, including axial temperature profile, radiative heat feedback, and burning rate, is measured and analyzed.

The whole burning process can be divided into three stages: 1) initial stage, 2) steady burning stage and 3) extinguishment stage. For the initial stage, the temperature in the tank and the radiative heat feedback from the flame to the fuel surface increase rapidly after ignition because the flame was mainly in the tank. Then these values gradually decrease and eventually stabilize, which is closely related to the flame base rise and ensuing stabilization. During the steady burning stage, the burning rate, flame height and axial temperature profile all remained stable. Then the fuel vapor layer and the down-reaching flame layer in the tank are distinguished based on the axial temperature profile. At the extinguishment stage, the flame re-enters the fuel tank, causing the axial temperature and the radiative heat feedback to the fuel surface increase in a short time, and then rapidly decrease.

During the steady burning stage, the down-reaching flame length (L_{down}) increases with the ullage height (h). Meanwhile, L_{down} increases significantly more for large tanks. Subsequently, an empirical exponential model ($L_{D,down}{*} = 0.58 \times h^{*1.46}$) is used to predict the dimensionless down-reaching flame length, which is also in good agreement with the experimental data from Dang et al.

Both the radiative heat feedback from the flame to the fuel surface and the burning rate decrease with the ullage height increase at the steady burning stage because of the flame base rise. Meanwhile, the decreasing rates are not obvious for the small-scale pool fires, because of the heat conduction effect from the side wall effect. By the analysis of the heat transfer process between flame and fuel surface, two processes are defined and then a burning rate model for pool fires with different ullage heights is established, which is in good agreement with the available experimental data in some extent.

The results and fundamental analysis can enhance the understanding of the radiative heat transfer process from the flame to the fuel surface. However, it is important to note that the developed correlation for the burning rate in this study is currently only valid for limited diameters of the stable pool fires with different ullage heights. Moreover, in practical fire accidents, the tank diameter is usually large and the corresponding accident scene is also complicated, which further affects burning behaviors and should be studied in future.

Acknowledgements

This work was supported by the Key Research and Development Program of National Fire and Rescue Administration (No. 2022XFZD04), the European Union's Horizon 2020 research and innovation programme (No. 952395) and the Fundamental Research Fund for the Central Universities (No. 2020QN05).

References

[1] G. Aydin, Production modeling in the oil and natural gas industry: an application of trend analysis, Petrol. Sci. Technol. 32.5 (2014). 555-564. https://doi.org/10.1080/10916466.2013.825271.

[2] L. Deng, F. Tang, X. Wang, Uncontrollable combustion characteristics of energy storage oil pool: Modelling of mass loss rate and flame merging time of annular pools, Energy. 224 (2021) 120181. https://doi.org/10.1016/j.energy.2021.120181.

[3] H. Paula, Insights from 595 tank farm fires from around the world, Process. Saf. Environ. Prot. 171 (2023) 773-782. https://doi.org/10.1016/j.psep.2023.01.058.

[4] Ministry of Emergency Management of the People's Republic of China, Investigation report on the "8.29" accident in Dalian Petrochemical Company. http://www.gov.cn/jrzg/2010-07/28/content_1665664.htm. (accessed 27 January 2023).

[5] V.I. Blinov, G.N. Khudyakov Diffusion Burning of Liquids, Army Engineer Research and Development Labs Fort Belvoir VA, 1961.

[6] X. Shi, A. K. Sahu, S. Nair, V. Raghavan, A.S. Rangwala, Effect of ullage on burning behavior of small-scale pool fires in a cavity, Proc. Combust. Inst. L. 36 (2017) 3113-3120. https://doi.org/10.1016/j.proci.2016.06.123.

[7] X. Shi, T. Raymond, S. Hayri, L. Nathan, Z. Leonard, S. Karen, A. S. Rangwala, Influence of ullage to cavity size ratio on in-situ burning of oil spills in ice infested water. Cold Reg. Sci. Technol. 140(2017)5-13. https://doi.org/10.1016/j.coldregions.2017.04.010

[8] E. A. Kolstad, V. Frette, U. Krause, B. Hagen. Lip-height effect in diffusive pool fires, Fire Saf. J. 125 (2021), 103428. https://doi.org/10.1016/j.firesaf.2021.103428.

[9] C. Kuang, L. Hu, X. Zhang, Y. Lin, L. W. Kostiuk, An experimental study on the burning rates of n-heptane pool fires with various lip heights in cross flow, Combust. Flame. 201 (2019) 93-103. https://doi.org/10.1016/j.combustflame.2018.12.011.

[10] C. Liu, L. Ding, M. Jangi, J. Jie, L. Yu, Effects of ullage height on heat feedback and combustion emission mechanisms of heptane pool fires, Fire Saf. J. 124 (2021) 103401. https://doi.org/10.1016/j.firesaf.2021.103401.

[11] L. Huang, N. Liu, W. Gao, J. Lei, X. Xie, L. Zhang, Lip height effects on pool fire: An experimental investigation, Proc. Combust. Inst. L. (2022). https://doi.org/10.1016/j.proci.2022.07.093.

[12] P. He, R. Xu, Q. Liu, P. Wang, X. Liu, C. Tao, The evolution of flame length for the oil tank fire with different top cover widths and lip heights, J. Loss. Prevent. Proc. 64 (2020) 104070. https://doi.org/10.1016/j.jlp.2020.104070.

[13] Z. Zhang, R. Zong, C. Tao, J. Ren, S. Lu, Experimental study on flame height of two oil tank fires under different lip heights and distances, Process. Saf. Environ. 139 (2020) 182-190. https://doi.org/10.1016/j.psep.2020.04.019.

[14] J. Zhao, X. Zhang, J. Zhang, W. Wang, C. Chen. Experimental study on the flame length and

burning behaviors of pool fires with different ullage heights, Energy, 246(2022) 123397. https://doi.org/10.1016/j.energy.2022.123397.

[15] C. Liu, M. Jangi, J. Ji, L. Yu, L. Ding, Experimental and numerical study of the effects of ullage height on plume flow and combustion characteristics of pool fires, Process. Saf. Environ, 151 (2021) 208-221. https://doi.org/10.1016/j.psep.2021.04.040.

[16] V. Babrauskas, Estimating large pool fire burning rates, Fire Technol. 19 (1983) 251–261. http://dx.doi.org/10.1007/BF02380810.

[17] A. Hamins, S. J. Fischer, T. Kashiwagi, M. E. Klassen, J. P. Gore, Heat feedback to the fuel surface in pool fires, Combust. Sci. Technol. 97 (1994), 37−62. https://doi.org/10.1080/00102209408935367.

[18] J. Zhao, X. Zhang, G. Song, H. Huang, J. Zhang, Experiments and modeling of the temperature profile of turbulent diffusion flames with large ullage heights. Fuel, 331 (2023) 125876. https://doi.org/10.1016/j.fuel.2022.125876.

[19] X. Dang, Y. He, J. Wang, Experimental study and numerical simulation on combustion behavior of pool fires with different lip heights. Journal of Fire Safety Science, 27 (2018) 213-221.10.3969/j.issn.1004-5309.2018.04.03.

[20] C. Liu, L. Ding, M. Jangi, J. Ji, L. Yu, H. Wan, Experimental study of the effect of ullage height on flame characteristics of pool fires, Combust. Flame. 216 (2020) 245-255. https://doi.org/10.1016/j.combustflame.2020.03.009.

[21] K. McGrattan, H. Baum, A. Hamins, Thermal radiation from large pool fires, NIST Interagency/Internal Report (NISTIR), 2000. https://doi.org/10.6028/NIST.IR.6546(accessed February 4, 2023).

[22] S. Sudheer, S. V. Prabhu, Measurement of flame emissivity of gasoline pool fires, Nucl. Eng. Des. 240 (2010) 3474−3480. https://doi.org/10.1016/j.nucengdes.2010.04.043.

[23] J. Wahlqvist, P. V. Hees, Implementation and validation of an environmental feedback pool fire model based on oxygen depletion and radiative feedback in FDS, Fire Saf. J. 85 (2016) 35-49. https://doi.org/10.1016/j.firesaf.2016.08.003.

[24] J. Chen, W. Li, X. Wan, Z. Lu, L. Zhang, W. Qi. Effect of dimensionless height of free tank wall on heat release rate. Fire. Technol, 32.03 (2013): 237-240. 10.3969/j.issn.1009-0029.2013.03.001.

[25] J. G. Quintiere, Fundamentals of fire phenomena, Wiley, West Sussex, 2006. 10.1002/0470091150.

[26] T. L. Bergman, S. L. Adrienne, F. P. Incropera, D. P. Dewitt, & Lavine, A. S. (2011), Fundamentals of heat and mass transfer. John Wiley & Sons.

Figure captions

Fig. 1. Schematic of the detailed experimental setup.

Fig. 2. Typical flame shapes at different times for the case D = 60 cm: (a) h^* = 0; (b) h^* = 1.0. Note that, apart from the first photo, the frames are taken at different times for the two conditions.

Fig. 3. Experimental data of burning rate and fuel mass for different ullage height vs. burning time (D = 60 cm: (a) h^* = 0; (b) h^* = 1.0).

Fig. 4. (a) Axial temperature profile in the vertical direction at different times (h^* = 1.0, D = 60 cm); (b) The radiative heat feedback from the flame to the fuel surface for different ullage heights (h^* = 0, 1.0, D = 60 cm) against the non-dimensional time.

Fig. 5. The axial temperature profile for steady burning with different ullage heights for the case D = 40 cm.

Fig. 6. A correlation of down-reaching flame length and dimensionless ullage height in the steady burning stage.

Fig. 7. Average radiative heat feedback versus h^* at the steady-state stage.

Fig. 8. Burning rates versus h^* at the steady burning stage.

Fig. 9. Illustrations of the flame radiative heat feedback and the heat transfer process simplifications. (1) Flame radiative heat feedback to the flame base; (2) Radiation from the flame base to the fuel surface.

Fig. 10. Comparison of experimental and calculated burning rate using Eq. (14) and experimental data in this work and from literature.